Journal of Solid State Chemistry 184 (2011) 2299–2305

Contents lists available at ScienceDirect

Journal of Solid State Chemistry

journal homepage: www.elsevier.com/locate/jssc

Preparation and formation mechanism of three-dimensionally ordered macroporous (3DOM) MgO, $MgSO_4$, $CaCO_3$, and $SrCO_3$, and photonic stop band properties of 3DOM $CaCO_3$

Masahiro Sadakane [a,*], Rika Kato [b], Toru Murayama [b], Wataru Ueda [b,**]

[a] Chemistry and Chemical Engineering, Graduate School of Engineering, Hiroshima University, 1-4-1, Kagamiyama, Higashi-Hiroshima, Hiroshima 739-8527, Japan
[b] Catalysis Research Center, Hokkaido University, N-21, W-10, Sapporo 001-0021, Japan

ARTICLE INFO

Article history:
Received 12 March 2011
Received in revised form
21 June 2011
Accepted 23 June 2011
Available online 1 July 2011

Keywords:
Macroporous material
Template method
Colloidal crystal
Photonic crystal

ABSTRACT

Three-dimensionally ordered macroporous (3DOM) magnesium (Mg) oxide (MgO), $MgSO_4$, calcium (Ca) carbonate ($CaCO_3$), and strontium (Sr) carbonate ($SrCO_3$) were prepared using a colloidal crystal of polymer spheres as a template. Ethanol or ethanol–water solution of metal salts (acetate or nitrate) and citric acid was infiltrated into the void of the colloidal crystal template of a monodispersed poly(methyl methacrylate) (PMMA) sphere. Heating of this PMMA–metal salt–citric acid composite produced the desired well-ordered 3DOM materials with a high pore fraction, which was confirmed by powder X-ray diffraction (XRD), scanning electron microscopy (SEM), transmission electron microscopy (TEM), and ultraviolet-visible (UV–vis) diffuse reflectance spectra. The presence of citric acid is crucial for production of the 3DOM structures. Reaction of citric acid with metal salt produces metal citrate solid in the void of PMMA spheres, which is necessary to maintain the 3DOM structure during the calcination process. 3DOM $CaCO_3$ shows opalescent colors because of it's photonic stop band properties.

1. Introduction

Fabrication of ordered porous materials in nano-scale order has been one of the most important topics in recent years, and much attention has been focused on three-dimensionally ordered macroporous (3DOM) materials with pores sized in the sub-micrometer range because of their applications in photonic crystals, catalysis, and separation [1–3]. 3DOM materials are produced by the following procedure: (i) a colloidal crystal template is prepared by ordering monodispersed spheres, e.g., polystyrene (PS), poly(methyl methacrylate) (PMMA) or silica, into a face-centered close-packed array (opal structure), (ii) interstices in the colloidal crystal are then filled with liquid metal precursors, either neat or in solution, which solidify in voids of the sphere templates, resulting in an intermediate composite structure, and (iii) an ordered form is produced after removing the template by calcination or extraction. The ordered ("inverse opals") structure synthesized using this method consists of a skeleton surrounding uniform close-packed macropores. The macropores are interconnected through windows that form as a result of contact between the template spheres prior to infiltration of the precursor solution. Furthermore, the 3DOM materials have high porosity, theoretically ca. 74%, which is attractive for catalyst and photonic materials.

Many 3DOM materials of metals, metal oxides, metal carbides, salts, and carbon have been prepared. However, 3DOM materials with group 2 elements of the periodic table [4], such as magnesium (Mg), calcium (Ca), and strontium (Sr), are rare. Alkaline properties of the group 2 elements are important factors influencing catalytic and adsorption properties. Therefore, 3DOM materials containing such elements are of great interest. Common metal precursors, such as nitrate or acetate salts, are not suitable for preparation of the 3DOM structure because of their melting temperature. These salts should be solidified at a temperature lower than the glass transition temperature of the polymer template, ca. 380 K for PMMA and PS, and not melt at a temperature at which the template polymer decomposes [5]. The first group 2 element containing 3DOM material, MgO and $CaCO_3$, was reported by Stein's group [6]. They infiltrated Mg acetate or Ca acetate into the void of a PS colloidal crystal template. Then the incorporated acetate was solidified as metal oxalate by reacting with oxalic acid in the void (2 step solidification method). Calcination of the PS-metal oxalate composite produced 3DOM MgO or $CaCO_3$. 3DOM single crystal of $CaCO_3$ was reported by Qi's [7]. They infiltrated amorphous calcium carbonate precursor into the void of colloidal crystal of poly (styrene–methyl methacrylate–acrylic acid) sphere. After calcination of the produced polymer–amorphous calcium carbonate precursor produced single crystal $CaCO_3$ with 3DOM structure. 3DOM MgO with additional mesopores was reported by

* Corresponding author. Fax: +81 82 424 5494.
** Corresponding author. Fax: 81 11 706 9163.
E-mail addresses: sadakane09@hiroshima-u.ac.jp (M. Sadakane), ueda@cat.hokudai.ac.jp (W. Ueda).

0022-4596/$ - see front matter © 2011 Elsevier Inc. All rights reserved.
doi:10.1016/j.jssc.2011.06.028

Dai's group [8]. They infiltrated an ethanol–water mixed solution of a mixture of Mg nitrate, citric acid, and Pluronic F127 ($EO_{106}PO_{70}EO_{106}$) into the void of a PMMA colloidal crystal. Calcination of the PMMA–Mg nitrate–citric acid composite produced 3DOM MgO. 3DOM MgF_2 and CaF_2 with large surface area and a strong Lewis acidity were reported by Kemnitz's group [9]. They infiltrated metal fluoride solution into the voids of PMMA spheres. After drying of the 3DOM metal fluoride–PMMA composite, the composite was washed with acetone or calcinated to produce 3DOM CaF_2 or MgF_2.

In this paper, we describe an easy preparation method, structural characterization, formation mechanism, and photonic properties of 3DOM materials with group 2 elements (Mg, Ca, and Sr). The main purpose is to understand the role of citric acid in the production of 3DOM MgO and to extend the preparation method to other group 2 elements such as Ca and Sr.

2. Experimental

2.1. Materials

All chemicals used were of reagent grade and they were used as supplied. Suspensions of monodispersed poly(methyl methacrylate) (PMMA) spheres (diameters: 240, 370, and 410 nm) were synthesized by literature techniques [10,11]. These spheres were packed into colloidal crystals by centrifugation. The obtained template was crushed with an agate mortar and the obtained particles were adjusted to 0.425–2.000 mm in size using testing sieves (Tokyo Screen, Co., LTD.) [10,11]. Quartz sand (10–15 mesh) was purchased from Kokusan Chemical Works (Tokyo).

2.2. Characterizations

Powder X-ray diffraction (XRD) patterns were recorded on a diffractometer (Rigaku, RINT UltimaIII) equipped with a graphite monochromator using Cu$K\alpha$ radiation (tube voltage: 40 kV, tube current: 20 mA). Diffraction line widths were obtained after subtraction of the instrumental width determined by the line width of silicon powder, and crystallite sizes were calculated from the width of the most intense lines using the Scherrer equation. Scanning electron microscopy (SEM) images were obtained with a JSM-7400 F (JEOL) or HD-2000 (Hitachi). Scanning transmission electron microscopy (STEM) images were obtained with an HD-2000 (Hitachi) using accelerating voltage of 200 kV. Samples for TEM were prepared by sonicating small amounts of the powder in 5 ml of ethanol for 1 min and then depositing a few drops of the suspension on a holey carbon grid. Nitrogen adsorption measurements were performed on an Autosorb 6 (Quantachrome, USA) sorption analyzer. Prior to the sorption measurements, the samples were degassed under vacuum at 473 K for 1 h. Surface areas were calculated by the Brunauer–Emmet–Teller (BET) method. Diffuse-Reflectance (DR) UV–vis spectra were obtained on a JASCO V-570 spectrophotometer equipped with an ISN-470 reflectance spectroscopy accessory. Samples were randomly oriented bulk powders. Thermamogravimetric-differential thermal analysis (TG-DTA) measurements were performed with a TG-8120 (Rigaku) thermogravimetric analyzer. Each sample was heated in air at a heating rate of 10 K min^{-1}. Temperature programmed desorption (TPD) measurement was performed with a TPD apparatus (BEL Japan Inc.) equipped with a Quadrupole mass spectrometer (M-100QA; Anelva). Elemental analyses were carried out by Instrumental Analysis Division, Equipment Management Center, Creative Research Institute, Hokkaido University.

Table 1
Summary of the preparation conditions and physicochemical properties of the obtained materials.[a]

Entry	Metal source[b] (amount)	Additive (amount)	Solvent (amount)	Calc. temp. (K)	3DOM structure[c]	Material[d], crystallite size (nm[e])	BET, surf. area ($m^2 g^{-1}$)
1	$Mg(OAc)_2$ (2.0 g)		EtOH (5 ml)–H_2O (5 ml)	673	C	MgO	
2	$Mg(NO_3)_2$ (1.13 g)		EtOH (5 ml)	673	C	MgO	
3	$Mg(NO_3)_2$ (1.28 g)	Ethylene glycol (ca. 0.5 ml)	MeOH (1 ml)	673	C	MgO	
4	$Mg(OAc)_2$ (2.15 g)	Citric acid (2.1 g)	EtOH (5 ml)–H_2O (5 ml)	773	A	MgO	
5	$Mg(NO_3)_2$ (1.13 g)	Citric acid (1.05 g)	EtOH (5 ml)	673	A	MgO	
6	$Mg(NO_3)_2$ (1.13 g)	Citric acid (1.05 g)	EtOH (1.5 ml)	673	A	MgO (6)	120
7	$Mg(NO_3)_2$ (1.13 g)	Citric acid (1.05 g)	EtOH (1.5 ml)	773	A	MgO (7)	100
8	$Mg(NO_3)_2$ (1.13 g)	Citric acid (1.05 g)	EtOH (1.5 ml)	873	A	MgO (9)	92
9	$Mg(NO_3)_2$ (1.13 g)	Citric acid (1.05 g)	EtOH (1.5 ml)	973	A	MgO (17)	61
10	$Mg(NO_3)_2$ (1.13 g)	Citric acid (1.05 g)	EtOH (1.5 ml)	1073	A	MgO (23)	53
11	$Mg(NO_3)_2$ (1.13 g)	Citric acid (1.05 g)	EtOH (1.5 ml)	1273	B	MgO	
12	$Mg(NO_3)_2$ (1.13 g)	Citric acid (1.05 g)	EtOH (1.5 ml)	1473	B	MgO	
13	$Mg_3(citrate)_2$ (0.90 g)	HCl	EtOH (1.5 ml)	773	A	MgO (9)	
14	$Mg_3(citrate)_2$ (0.90 g)	HNO_3	EtOH (1.5 ml)	773	A	MgO (9)	
15	$Mg_3(citrate)_2$ (0.90 g)	H_2SO_4	EtOH (1.5 ml)	773	A	$MgSO_4$ (8)	36
16	$Ca(NO_3)_2$ (1.18 g)	Citric acid (1.05 g)	MeOH (1.5 ml)–H_2O (3.5 ml)	673	A	$CaCO_3$ (Calcite) (18)	59
17	$Ca(NO_3)_2$ (1.18 g)	Citric acid (1.05 g)	MeOH (1.5 ml)–H_2O (3.5 ml)	773	D	$CaCO_3$ (Calcite) (31)	23
18	$Ca(NO_3)_2$ (1.18 g)	Citric acid (1.05 g)	MeOH (1.5 ml)–H_2O (3.5 ml)	873	D	$CaCO_3$ (Calcite (39)+Vaterite)	21
19	$Sr(NO_3)_2$ (1.06 g)	Citric acid (1.05 g)	MeOH (1.5 ml)–H_2O (3.5 ml)	673	A	$SrCO_3$ (12)	54
20	$Sr(NO_3)_2$ (1.06 g)	Citric acid (1.05 g)	MeOH (1.5 ml)–H_2O (3.5 ml)	773	C	$SrCO_3$ (20)	33
21	$Sr(NO_3)_2$ (1.06 g)	Citric acid (1.05 g)	MeOH (1.5 ml)–H_2O (3.5 ml)	873	D	$SrCO_3$ (34)	28

[a] PMMA with a diameter of 240 nm was used.

[b] All compounds were hydrate compounds: $Mg(NO_3)\cdot 6H_2O$, $Mg(OAc)_2\cdot 4H_2O$, $Mg_3(citrate)_2\cdot 9H_2O$, $Ca(NO_3)_2\cdot 4H_2O$, $Sr(NO_3)_2\cdot 4H_2O$.

[c] A. Well-ordered 3DOM structure was observed by SEM, and the fraction of 3DOM structure was more than 95% (More than 20 particles were randomly chosen by SEM, and images with magnifications of 5000–10000 were taken. The fraction of 3DOM structure was calculated as follows: number of particles that contain the 3DOM structure/total number of particles). B. The fraction of 3DOM structure was more than 90%, but the 3DOM structure was not well-ordered. C. 3DOM structure was only partially found, the fraction of 3DOM being less than 10%. D. No 3DOM structure was observed by SEM.

[d] Crystal structure was determined by powder-XRD. MgO (JCPDS: 045–0946), $CaCO_3$ (calcite, JCPDS: 047–1743), $CaCO_3$ (vaterite, JCPDS: 033-0268), $SrCO_3$ (JCPDS: 005–0418), $MgSO_4$ (JCPDS: 021–0546).

[e] Crystallite sizes were calculated from the width of the most intense line using the Scherrer equation.

2.3. Synthesis of 3DOM MgO

Magnesium nitrate hydrate ($Mg(NO_3)_2 \cdot 6H_2O$, 1.13 g) and citric acid (1.05 g) were dissolved with ca. 1.5 ml of ethanol. Then PMMA colloidal crystals were soaked in the solution for 3 h. Excess solution was removed from the impregnated PMMA colloidal crystals by vacuum filtration. The obtained sample was allowed to dry in air at room temperature overnight. A 0.5-g amount of the sample was mixed with 2.5 g of quartz sand (10 – 15 mesh) and calcined in a tubular furnace (inner diameter of ca. 21 mm) in an air flow (50 ml min^{-1}). The temperature was raised at a rate of 1 K min^{-1} to 873–1073 K and held for 5 h.

2.4. Synthesis of 3DOM $CaCO_3$ and $SrCO_3$

Metal nitrate hydrate ($Ca(NO_3)_2 \cdot 6H_2O$, 1.18 g or $Sr(NO_3)_2 \cdot 6H_2O$, 1.06 g) and citric acid (1.05 g) were dissolved in ca. 1.5 ml of methanol and 3.5 ml of water. Then PMMA colloidal crystals were soaked in the solution for 3 h. Excess solution was removed from the impregnated PMMA colloidal crystals by vacuum filtration. The obtained sample was allowed to dry in air at room temperature overnight. A 0.5-g amount of the sample was mixed with 2.5 g of quartz sand (10 – 15 mesh) and calcined in a tubular furnace (inner diameter of ca. 21 mm) in an air flow (50 ml min^{-1}). The temperature was raised at a rate of 1 K min^{-1} to 673 K and held for 5 h.

2.5. Synthesis of $CaCO_3$ without PMMA template

Calcium nitrate hydrate ($Ca(NO_3)_2 \cdot 6H_2O$, 1.18 g) and citric acid (1.05 g) were dissolved in ca. 1.5 ml of methanol and 3.5 ml of water. This solution was heated in a muffle oven. The temperature was raised at a rate of 1 K min^{-1} to 673 K and held for 5 h.

3. Results and discussion

3.1. Preparation and formation mechanism of 3DOM MgO

$Mg(NO_3)_2$ and $Mg(OAc)_2$ were not suitable as starting materials for preparation of a 3-dimensionally ordered macroporous (3DOM) structure [6] (Table 1, Entries 1 and 2). We previously reported that our method using ethylene glycol could not produce 3DOM MgO material (Table 1, Entry 3) [5]. However, by adding

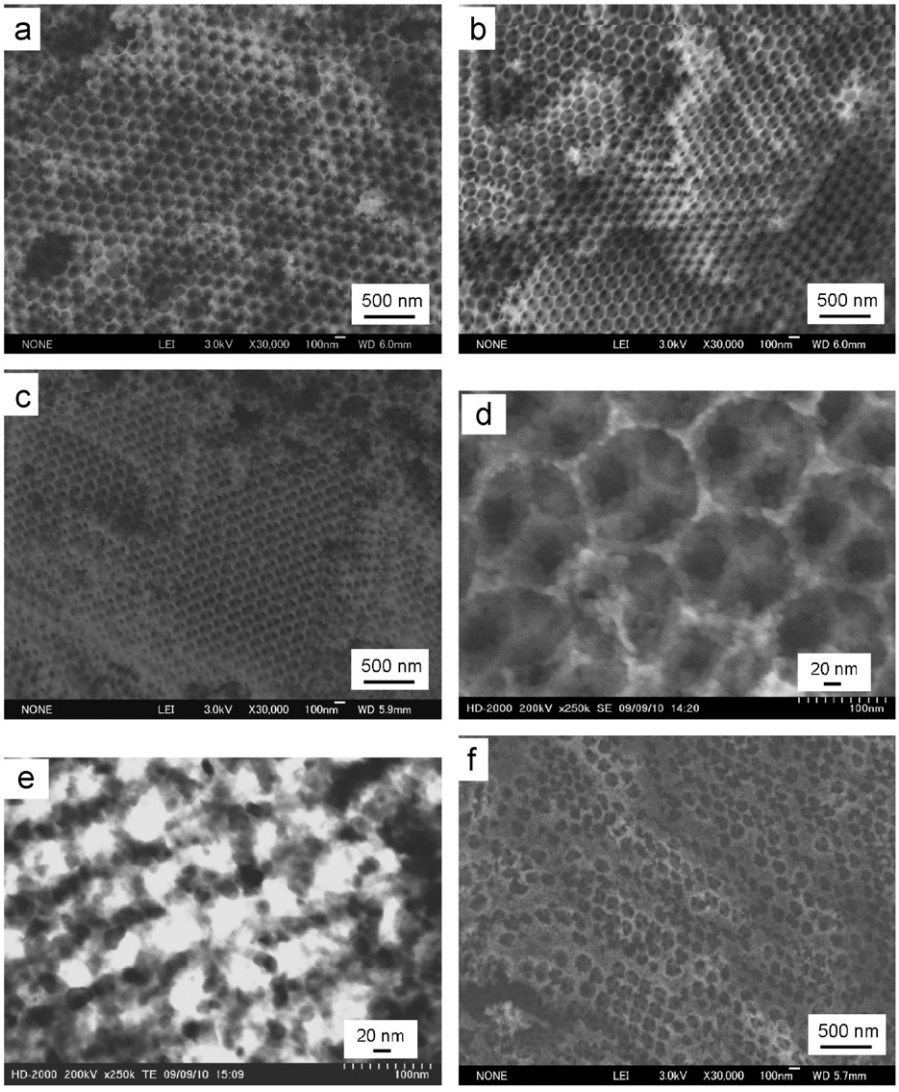

Fig. 1. SEM and TEM images of 3DOM MgO prepared using colloidal crystal templates of PMMA (diameter of 240 nm). SEM image of sample prepared using $Mg(NO_3)_2$-citric acid ethanol solution. Calcination temperature was 773 K (a). Sample prepared using $Mg(OAc)_2$-citric acid ethanol–water solution. Calcination temperature was 773 K (b). SEM and TEM images of sample prepared using $Mg(NO_3)_2$-citric acid ethanol solution. Calcination temperatures were 973 K (c), (d), (e). SEM image of sample prepared using $Mg(NO_3)_2$-citric acid ethanol solution. Calcination temperature was 1473 K (f).

citric acid to $Mg(NO_3)_2$ or $Mg(OAc)_2$ solution, a 3DOM structure was successfully obtained (Table 1, Entries 4–6, Fig. 1(a) and (b)). Recently, Dai's group also reported preparation of 3DOM MgO using ethanol solution of $Mg(NO_3)_2$ with citric acid [8]. We have clearly indicated that $Mg(OAc)_2$ is also a suitable Mg precursor. The well-ordered 3DOM structure was stable at temperatures up to 1073 K (Table 1, Entries 4–10, Fig. 1(c)). After calcination at these temperatures, crystalline MgO was obtained (Fig. 2). Crystallite sizes estimated by XRD of 3DOM MgO prepared at 973 K were ca. 17 nm (Table 1, Entry 9), which is similar to wall thickness (Fig. 1(e)). These small crystallites constructed 3DOM walls similar to 3DOM iron based oxide [11,12]. By increasing the calcination temperature, crystallite size was increased and surface area was decreased. When the temperature was higher than 1273 K, non-well-ordered 3DOM MgO was obtained due to sintering of crystallites (Fig. 1(f) and Entries 11 and 12).

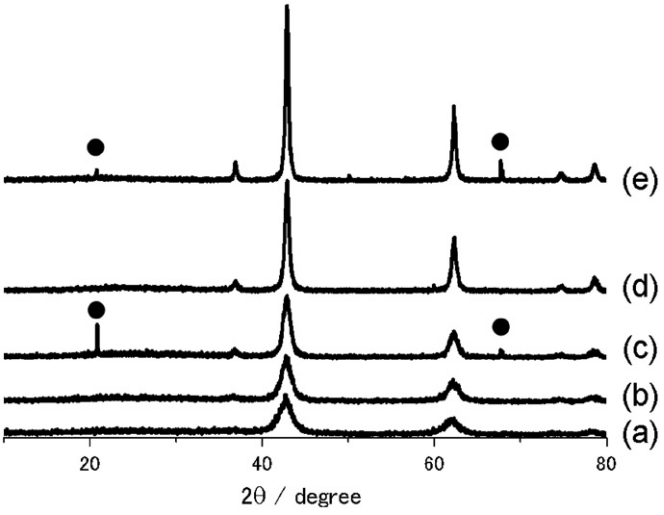

Fig. 2. XRD of 3DOM MgO prepared using colloidal crystal templates of PMMA (diameter of 240 nm). Calcination temperatures were 673 K (a), 773 K (b), 873 K (c), 973 K (d), and 1073 K (e). Closed circles indicate diffractions corresponding to quartz, which was used for calcination.

Fig. 3(a) shows TG-DTA curves of $Mg(NO_3)_2$ and citric acid dissolved in ethanol. Gradual weight loss was observed up to 600 K, and an exothermic weight loss was observed at temperatures between ca. 700 and 760 K. This TG-DTA behavior indicates that $Mg(NO_3)_2$ reacted with citric acid at a temperature below 430 K, because an endothermic weight loss at 430 K shown in TG-DTA of citric acid (Fig. 3(c)) and an endothermic weight loss at ca. 700 K shown in TG-DTA of $Mg(NO_3)_2$ (Fig. 3(b)) were not observed. Table 2 summarizes results of elemental analysis of material obtained after heating $Mg(NO_3)_2$ and citric acid dissolved in ethanol at different temperatures. C, H, and N contents changed at temperatures from 323 to 423 K (Table 2, Entries 1 and 2) but did not change at heating temperatures higher than 423 K (Table 2, Entries 3–5). N content decreased from 323 to 373 K, and N was completely removed at a temperature of 423 K, indicating that nitrate removal started at a temperature lower than 373 K and was completed at a temperature of 423 K. The IR spectrum of material obtained after heating of

Table 2
Elemental analysis of solid material obtained after heating of ethanol solution of $Mg(NO_3)_2$ and citric acid at different temperatures.

Entry	Temp. (K)	Elemental analysis (%)		
		C	H	N
1	323	21	4.8	4.1
2	373	23	4.8	3.3
3	423	32	3.7	0
4	473	31	3.8	0
5	573	30	3.5	0

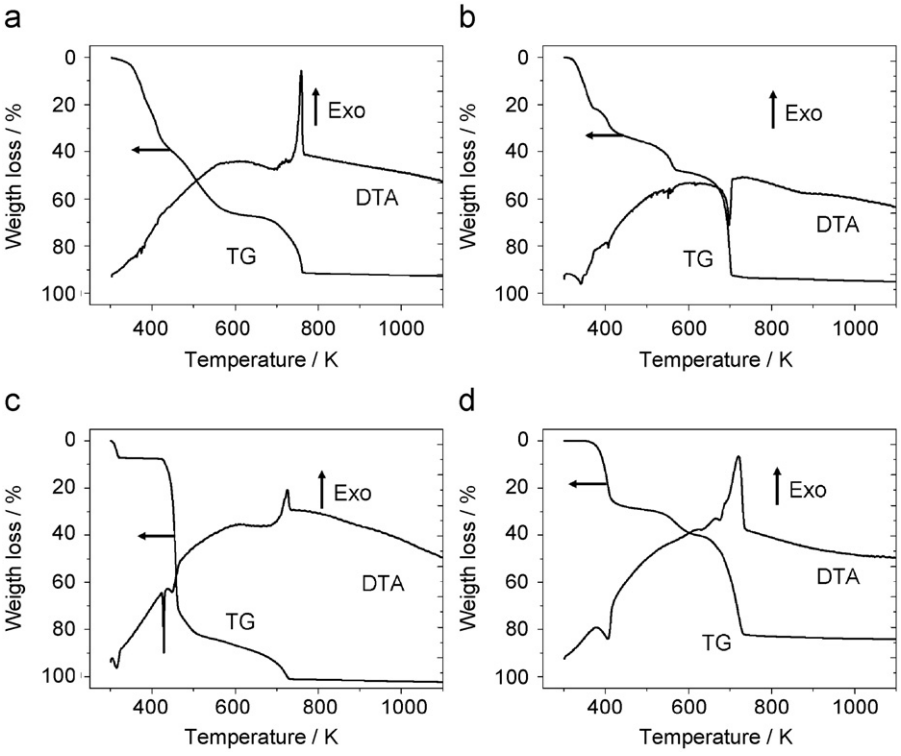

Fig. 3. TG-DTA curves of $Mg(NO_3)_2$–citric acid ethanol solution (a), $Mg(NO_3)_2$ (b), citric acid (c), and $Mg_3(citrate)_2$ (d).

$Mg(NO_3)_2$ and citric acid dissolved in ethanol at 423 K shows carbonyl peaks, which was also observed in the IR spectrum of $Mg_3(citrate)_2$ (Figure S1). TG-DTA of $Mg_3(citrate)_2$ shows an exothermic weight loss at ca. 700 K (Fig. 3(d)). These results indicate that heating of ethanol solution of $Mg(NO_3)_2$ and citric acid produced Mg citrate solid in the void of the PMMA template at 423 K. In order to maintain the 3DOM structure, solidification should occur at a temperature lower than the glass transition temperature (ca. 378 K) of PMMA [5]. Reaction of Mg nitrate with citric acid started at a temperature lower than 373 K. Therefore, we propose solidification of $Mg(NO_3)_2$ started at a temperature lower than 378 K (glass transition temperature of PMMA) in the presence of citric acid. Li's group reported that citric acid is crucial for preparation of 3DOM CeO_2 and La_2O_3 [13]. They reported that the chelating effect of citric acid facilitated the formation of a 3DOM structure.

Commercially available $Mg_3(citrate)_2$ can also be used as a starting material. $Mg_3(citrate)_2$ has low solubility in ethanol, and acids were added to increase solubility. 3DOM MgO was obtained using ethanol solution of $Mg_3(citrate)_2$ with HCl or HNO_3 (Table 1, Entries 13 and 14, and Figure S2), and 3DOM $MgSO_4$ was obtained using ethanol solution of $Mg_3(citrate)_2$ with H_2SO_4 (Table 1, Entry 15, and Figures S2 and S3). This is the first report on production of a 3DOM $MgSO_4$ material. Crystallite size of 3DOM $MgSO_4$ estimated by XRD was ca. 8 nm, which is similar to crystallite sizes (7–9 nm) of 3DOM MgO at same calcination temperature (Table 1, Entries 7, 13–15). However, surface area of 3DOM $MgSO_4$ was surprisingly smaller than that of 3DOM MgO, and we are now investigating reasons. IR spectra of 3DOM MgO materials show a peak corresponding to CO_3^{2-}, which form on the surface of MgO by a reaction of basic MgO with CO_2 (Figure S4). On the other hand, IR spectrum of 3DOM $MgSO_4$ shows no peak corresponds to CO_3^{2-} but peak corresponds to SO_4^{2-} (Figure S4(e)) because surface of $MgSO_4$ is not basic and does not react with CO_2.

3.2. Preparation of 3DOM $CaCO_3$ and $SrCO_3$

$Sr(NO_3)_2$ or $Ca(NO_3)_2$ was used as a starting compound to prepare 3DOM material with Sr or Ca. For both cases, well-ordered 3DOM $CaCO_3$ or $SrCO_3$ was produced after calcination at 673 K (Table 1, Entries 16 and 19, Figs. 4(a), (d), (e), (f), (i), (j), and 5). Heating at higher temperature resulted in collapse of the 3DOM structure due to crystal growth (Table 1, Entries 17, 18, 20, 21, and Fig. 4 (b), (c), (g), (h)).

TG-DTA analysis of 3DOM $CaCO_3$ material prepared after calcination at 673 K showed an exothermic weight loss starting at ca. 673 K and an endothermic weight loss starting at ca. 873 K (Figure S4(a)). The first exothermic weight loss corresponded to combustion of organic residue from PMMA, because this exothermic weight loss is not observed in TG-DTA of $CaCO_3$ prepared at 673 K without a PMMA template (Figure S4(c)). The endothermic weight loss corresponded to decomposition of $CaCO_3$ to CaO. Evolution of CO_2 and H_2O at the first exothermic weight loss and evolution of CO_2 were confirmed by temperature programmed desorption (TPD) analysis (Figure S5(b) and (d)). Decomposition of $SrCO_3$ to SrO started at ca. 1000 K (Figure S6).

3.3. Photonic properties

The colors of 3DOM $CaCO_3$ prepared using PMMA with diameters of 240, 370 and 410 nm (Fig 4 (a), (d), and (e)) were opalescent violet, blue and green, respectively, under room light, which is visible evidence of their long-range 3D order (Fig. 6). The 3DOM $CaCO_3$ materials were characterized using DR UV–vis spectroscopy (Fig. 7), and photonic stop bands centered at 440, 492 and 526 nm corresponding to violet, blue and green colors, respectively, were observed. 3DOM $CaCO_3$ was first reported by Stein's group [6], but photonic stop bands and opalescent colors were not reported.

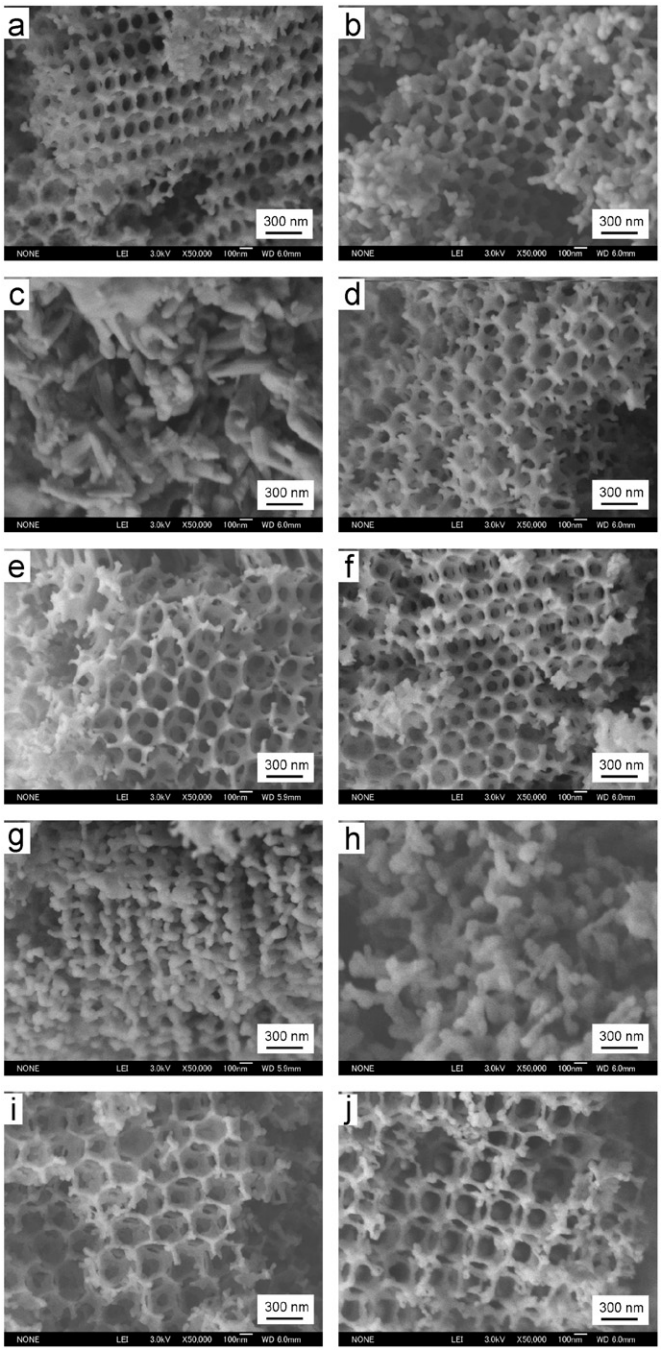

Fig. 4. SEM images of $CaCO_3$ and $SrCO_3$ prepared using colloidal crystal templates of PMMA. $CaCO_3$ materials prepared using PMMA with a diameter of 240 nm. Calcination temperatures were 673 K (a), 773 K (b) and 873 K (c). $CaCO_3$ materials prepared using PMMA with a diameter of 370 nm. Calcination temperature was 673 K (d). $CaCO_3$ materials prepared using PMMA with a diameter of 410 nm. Calcination temperature was 673 K (e). $SrCO_3$ materials prepared using PMMA with a diameter of 240 nm. Calcination temperatures were 673 K (f), 773 K (g) and 873 K (h). $SrCO_3$ materials prepared using PMMA with a diameter of 370 nm. Calcination temperature was 673 K (i). $SrCO_3$ materials prepared using PMMA with a diameter of 410 nm. Calcination temperature was 673 K (j).

An approximate expression for the position of the stop band is given by

$$\lambda = 2d_{hkl}n_{avg}, \quad (1)$$

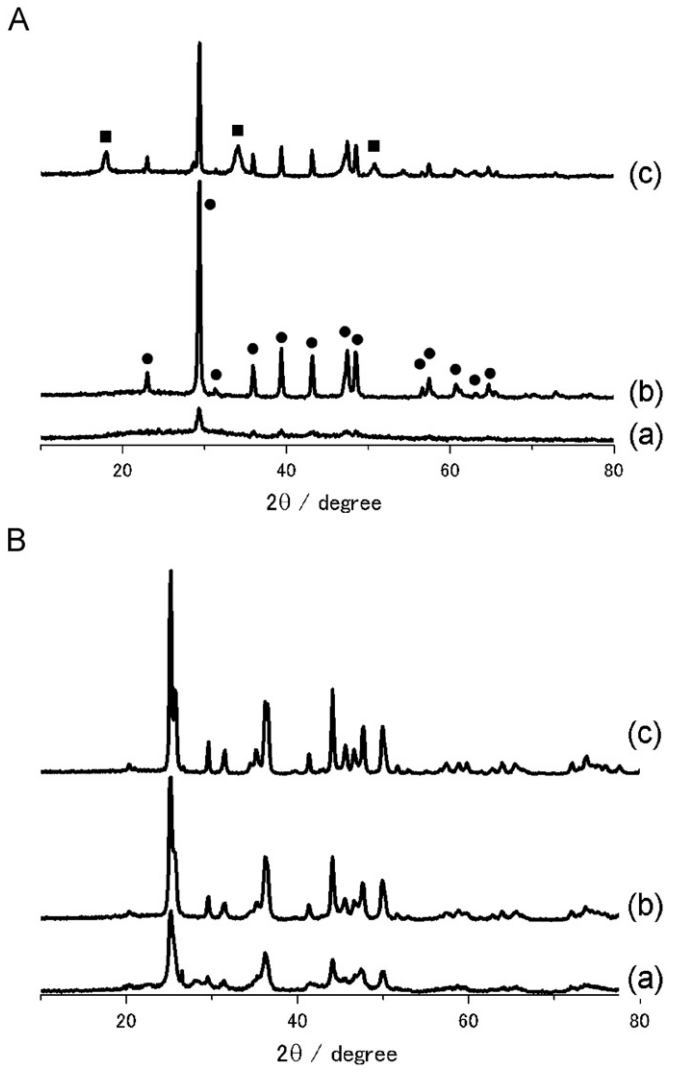

Fig. 5. XRD of $CaCO_3$ (A) and $SrCO_3$ (B) materials prepared using a colloidal crystal template of PMMA with a diameter of 240 nm. Calcination temperatures were 673 K (a), 773 K (b) and 873 K (c). Closed circles and squares indicate diffraction corresponding to calcite (JCPDS: 047–1743) and vatelite (JCPDS: 033-0268) , respectively.

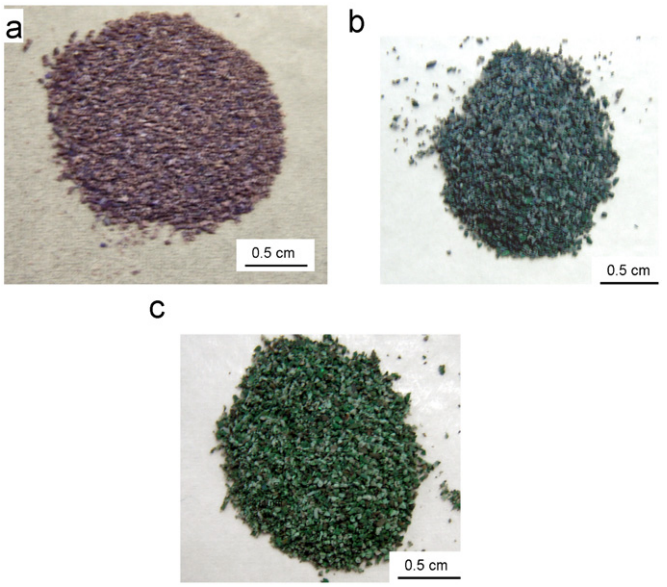

Fig. 6. Photographs of 3DOM $CaCO_3$ prepared using PMMA templates with diameters of 240 nm (a), 370 nm (b), and 410 nm (c). Calcination temperature was 673 K.

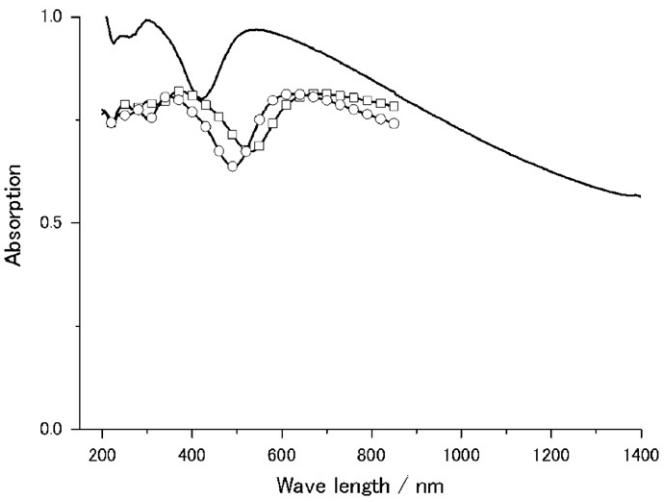

Fig. 7. Absorption spectra of 3DOM $CaCO_3$ prepared using PMMA templates with diameters of 240 nm (solid line), 370 nm (solid line with open circles), and 410 nm (solid line with open squares). Calcination temperature was 673 K.

where λ is the wavelength of the stop band minimum, d_{hkl} is the interplanar spacing, and n_{avg} is the average refractive index of the materials [10,14]. n_{avg} is given by

$$n_{avg} = \{(1-a)n_{wall}^2 + a n_{void}^2\}^{1/2}, \quad (2)$$

where a is pore fraction of the material, n_{wall} is refractive index of $CaCO_3$, and n_{void} is refractive index of air ($n_{void}=1.00$). The interplanar spacing of the (1 1 1) set planes d_{111} is given by

$$d_{111} = (2/3)^{1/2} D, \quad (3)$$

where D is pore size.

Pore sizes (D) of 3DOM $CaCO_3$ prepared using PMMA spheres with diameter of 240, 370 and 411 nm were 190, 270 and 309 nm, respectively. The pore size is usually smaller than the original PMMA sphere diameter because of shrinkage caused by melting of PMMA, crystallization of walls, and removal of chelating materials. The photonic stop band position is tunable by changing PMMA diameter.

As shown in Eqs. (1)–(3), stop band wavelength depends on the refractive index of the materials, pore fractions, and pore diameter. 3DOM MgO, $MgSO_4$, and $SrCO_3$ did not show clear opal opalescent color, because their stop band wavelength was not in the visible light range.

4. Conclusion

Well-ordered 3DOM MgO, $MgSO_4$, $CaCO_3$, and $SrCO_3$ materials were obtained using a colloidal crystal template method in a high pore fraction. The presence of citric acid in metal salt solution is crucial for production of a 3DOM structure. The citric acid reacts with the metal cation to form metal–citrate solid in the void of the colloidal crystal. High porosity and high order of the 3DOM materials, which are attractive features for application as future catalysts, filters and electrode material, were confirmed by using SEM, TEM, and photonic stop band properties.

Acknowledgments

We thank Mitsubishi Rayon Co. for financial support and useful discussion about synthesis of PMMA spheres.

Appendix A. Supplementary materials

Supplementary data associated with this article can be found in the online version at doi:10.1016/j.jssc.2011.06.028.

References

[1] A. Stein, F. Li, N.R. Denny, Chem. Mater. 20 (2008) 649–666.
[2] R.C. Schroden, A. Stein, 3D Ordered Macroporous Materials, Wiley-VCH Verlag, Weinheim, Germany, 2004.
[3] M. Sadakane, W. Ueda, in: D.W. Bruce, D. O'Hare, R.I. Walton (Eds.), Porous Materials, John Wiley & Sons Ltd, West Sussex, 2011, pp. 147–216.
[4] G.J. Leigh, Nomenclature of Inorganic Chemistry: Recommendations. 1990.
[5] M. Sadakane, T. Horiuchi, N. Kato, C. Takahashi, W. Ueda, Chem. Mater. 19 (2007) 5779–5785.
[6] H. Yan, C.F. Blanford, B.T. Holland, W.H. Smyrl, A. Stein, Chem. Mater. 12 (2000) 1134–1141.
[7] C. Li, L. Qi, Angew. Chem. Int. Ed. 47 (2008) 2388–2393.
[8] H. Li, L. Zhang, H. Dai, H. He, Inorg. Chem. 48 (2009) 4421–4434.
[9] J. Noack, K. Teinz, C. Schaumberg, C. Fritz, S. Rüdiger, E. Kemnitz, J. Mater. Chem. 21 (2010) 334–338.
[10] M. Sadakane, T. Horiuchi, N. Kato, K. Sasaki, W. Ueda, J. Solid State Chem. 183 (2010) 1365–1371.
[11] M. Sadakane, C. Takahashi, N. Kato, H. Ogihara, Y. Nodasaka, Y. Doi, Y. Hinatsu, W. Ueda, Bull. Chem. Soc. Jpn. 80 (2007) 677–685.
[12] M. Sadakane, C. Takahashi, N. Kato, T. Asanuma, H. Ogihara, W. Ueda, Chem. Lett. 35 (2006) 480–481.
[13] Q.Z. Wu, S.Y., J.F. Liao, T.G. Li, Mater. Lett. 58 (2004) 2688–2691.
[14] C.I. Aguirre, E. Reguera, A. Stein, Adv. Funct. Mater. 20 (2010) 2565–2578.